HHS Public Access

Author manuscript

J Chem Inf Comput Sci. Author manuscript; available in PMC 2024 January 22.

Published in final edited form as:

J Chem Inf Comput Sci. 1998 ; 38(6): 1239–1248. doi:10.1021/ci980080e.

Molecular Modeling Studies of Human A_3 Adenosine Antagonists: Structural Homology and Receptor Docking

Stefano Moro,

An-Hu Li,

Kenneth A. Jacobson*

Molecular Recognition Section, Laboratory of Bioorganic Chemistry, National Institute of Diabetes, Digestive and Kidney Diseases, National Institutes of Health, Bethesda, Maryland 20892-0810

Abstract

Molecular modeling studies were conducted on various chemically diverse classes of human A_3 adenosine receptor antagonists (hA3ANTs), such as adenines, xanthines, triazoloquinazolines, flavonoids, thiazolo-pyridines, 6-phenyl-1,4-dihydropyridines, and 6-phenylpyridines. Using a combination of ab initio quantum mechanical calculations, electrostatic potential map comparison, and the steric and electrostatic alignment (SEAL) method, a general pharmacophore map for hA3ANTs has been derived. Based on the proposed pharmacophore map, we hypothesize that the receptor binding properties of different A_3 antagonist derivatives are due to recognition at a common region inside the receptor binding site and, consequently, a common electrostatic potential profde. A model of the human A_3 receptor, docked with the triazoloquinazoline reference ligand CGS 15953 (9-chloro-2-(2-furyl)[l,2,4]triazolo[1,5-*c*]quinazolin-5-amine), was built and analyzed to help interpret these results. All other antagonist structures were docked inside the receptor according to the results obtained through the steric and electrostatic alignment (SEAL) approach using the structure of CGS 15953 as a template. The receptor model was derived from primary sequence comparison, secondary structure predictions, and three-dimensional homology building, using rhodopsin as a template. An energetically refined 3D structure of the ligand—receptor complex was obtained using our recently introduced *cross-docking* procedure *(J. Med. Chem.* **1998,** *41,* 1456–1466), which simulates the ligand-induced reorganization of the native receptor structure.

1. INTRODUCTION

Selective antagonists have been reported for adenosine A_1, A_{2A}, and A_3 receptors,[1] which are members of the G protein-coupled superfamily characterized by seven transmembrane helical domains (TMs). Activation of the A_3 receptor has been linked to stimulation of phospholipases C[2] and D[3] and inhibition of adenylyl cyclase.[1] Antagonists for the A_3 adenosine receptor are sought as potential antiinflammatory, antiasthmatic, or antiischemic agents.[4–8] The A_3 receptor has a unique pharmacology [4,9–11] Most strikingly, xanthines,

* Correspondence to Dr. K. A. Jacobson, Chief, Molecular Recognition Section, LBC, NIDDK, NIH, Bldg. 8A, Rm. B1A-19, Bethesda, MD 20892-0810. tel.:(301) 496-9024. fax:(301) 480-8422. kajacobs@helix.nih.gov.

such as caffeine and theophylline, which have provided versatile leads for antagonists at other adenosine receptor subtypes, are much less potent at the A_3 receptor. Furthermore, there are major species differences in the affinity of antagonists, e.g. typically many antagonists have 1–2 orders of magnitude greater affinity at human vs rat A_3 receptors.

Potent and selective A_3 receptor antagonists were unknown until recently.[4] In fact, the attempt to design A_3 selective adenine or xanthine derivatives by applying the structural principles of recognition derived from A_1 and A_{2A} studies has not resulted in highly potent and selective compounds. For example, one of the most potent xanthine derivatives binding at human A_3 receptors, BWA 1433 (Figure 1), has a K_i, value of 54 nM but is not selective for this subtype (K_i, at A_1 receptors = 20 nM).[11] Recently, Camaioni et al. have further explored the affinity of adenine derivatives and found that the presence of an 8-alkynyl group resulted in A_3 receptor affinity in the submicromolar range (K_i = 620 nM).[12]

We have introduced A_3 receptor antagonists belonging to four distinct, nonpurine chemical classes (Figure 1). A broad screening of phytochemicals has demonstrated that certain flavone, flavonol, and flavanone derivatives have micromolar affinity at A_3 receptors. This finding has been subjected to chemical optimization leading to 3,6-dichloro-2′-isopropyl-oxy-4′-methyl-flavone (MRS 1067, K_i = 561 nM), which is both relatively potent and highly selective (200-fold) for human A_3 vs human A_1 receptors.[13]

Similarly 9-chloro-2-(2-furyl)-5-phenylacetyamino[1,2,4]-triazolo[1,5-*c*]quinazoline (MRS1220), a derivative of the triazoloquinazoline antagonist CGS 15943 (Figure 1), was found to selectively displace radioligand from human A_3 receptors with a K_i) value of 0.65 nM.[14] The *N*-phenylacetyl group of MRS 1220 is the key to its selectivity (470-fold vs rat A_1 and 80-fold vs rat A_{2A} receptors) and extremely high potency at A_3 receptors.[15]

Also, 1,4-dihydropyridine derivatives, such as the known L-type Ca^{2+} channel antagonists niguldipine and nicardipine, demonstrated micromolar affinity at human A_3 receptor.[16] Chemical optimization of this class of antagonists has resulted in derivatives such as 3,5-diethyl-2-methyl-6-phenyl-4-[2-phenyl-(*E*)-vinyl]-l,4-(±)-dihydropyridine-3,5-dicar-boxylate (MRS 1097), which is 200-fold more selective in binding to human A_3 receptor than human A_1 receptors (K_i; = 0.108 nM), and does not bind to Ca^{2+} channels.[16] We have synthesized a new generation of dihydropyridine antagonists with A_3 receptor selectivities of >30 000-fold.[17]

Finally, we have studied a new class of pyridine derivatives, all of which were obtained through oxidation of 1,4-dihydropyridines, and identified combinations of substituents resulting in high selectivity for human A_3 receptors.[18] The pyridine 2,3,4,5-tetraethyl-6-phenylpyridine-3-thiocarboxylate-5-carboxylate (MRS 1476, Figure 1) is a potent (K_i = 20 nM) and highly selective antagonist (> 3000-fold) for human A_3 vs rat A_1 receptors.[18]

Other A_3 receptor antagonists L-249,313 (6-carboxymethy-5,9-dihydro-9-methyl-2-phenyl[l,2,4]triazolo[5,l-*a*]-[2,7]naphthyridine) and L-268,605 (3-(4-methoxyphenyl)-5-amino-7-oxothiazolo[3,2]pyrimidine (Figure 1) have been identified through broad screening by M. Jacobson et al. at Merck.[19] L-249,313 was shown to be noncompetitive in binding (K_i, = 13 nM), while L-268,605 is a competitive antagonist (K_i = 18 nM).[19]

The peculiarity of the A_3 antagonist family is its apparent lack of common chemical or structural characteristics, but despite the apparent structural diversity of hA3ANTs, certain common electronic and steric features have become apparent through a combination of ab initio quantum mechanical calculations, electrostatic potential map comparison, and steric and electrostatic alignment (SEAL) analysis. In the present study we provide evidence for a possible common binding site for all these classes of hA3ANTs.

2. MATERIALS AND METHODS

2.1. Molecular Modeling.

All calculations were performed on a Silicon Graphics Indigo 2 R8000 workstation.

All antagonist models were constructed using the "Sketch Molecule" of SYBYL 6.3.[20] Semiempirical molecular orbital calculations were done using the AMI Hamiltonian[21] as implemented in MOPAC 6.0[22] (keywords: PREC, GNORM = 0.1, EF, MMOK if necessary); these calculation were carried out to provide reasonable initial geometries for ab initio molecular orbital calculations.

All ab initio molecular orbital calculations were carried out using Gaussian 94.[23] Geometry optimizations were performed at the Hartree–Fock (HF) level using the 3–21G-(*) basis set.[24] Vibrational frequency analysis was used to characterize the minima stationary points (zero imaginary frequencies). Atomic charges were calculated by fitting to electrostatic potential maps (CHELPG method).[24] Electrostatic contours were generated using standard procedures within SYBYL.

Superimposition of these geometry-optimized antagonist structures was carried out using the steric and electrostatic alignment (SEAL)[26] method implemented in PowerFit v.1.0[27] on a 166 MHz Pentium PC. Starting with 250 random orientations, the steric volume and the partial atomic charges of pairwise molecular structures were used by SEAL in determining their optimal alignments. We used the following parameters for A_3 antagonist alignments with SEAL: $\alpha = 0.5$, $W_S = 1$, $W_E = 1$, $W_{AM} = 1$ with the Gaussian attenuation function.

The three-dimensional human A_3 receptor model was built and optimized using SYBYL 6.3 and Macromodel 5.0,[28] respectively, based on the approach described by van Rhee et al.[29] and Moro et al.[30] Briefly, the seven transmembrane helical domains were identified with the aid of Kyte–Doolittle hydrophobicity[31] and E_{mini}[31] surface probability parameters. The helices were built and energy minimized for each transmembrane sequence. The minimized helices were then grouped together to form a helical bundle matching the overall characteristics of the electron density map of rhodopsin. The helical bundle was energy minimized using the AMBER[32] all-atom force field, until the *rms* value of the conjugate gradient (CG) was < 0.1 kcal/mol/Å. A fixed dielectric constant = 4.0 was used throughout these calculations.

All A_3 antagonist models were rigidly docked into the helical bundle using graphical manipulation with continuous energy monitoring (Dock module of SYBYL). The manually docked local energy minimized receptor–ligand complexes were subjected to an additional

coniugate gradient (CG) minimization run of 300 steps. Partial atomic charges for the ligands were taken from the Gaussian output files. A fixed dielectric constant = 4.0 was used throughout the docking calculations. We have recently introduced the *cross-docking* procedure to obtain energetically refined structures of $P2Y_1$ receptor–ligand complexes.[30] We applied this technique to predict the structure of the MRS 15943-A_3 receptor complex. Cross docking allows possible ligand-induced rearrangements of the 7TM bundle to be explored by sampling 7TM conformations in the presence of the docked ligands. Small translations and rotations were applied to each helix relative to its original position until a new lower energy geometry was obtained. These manual adjustments were followed by 25 ps of molecular dynamics (MD module of Macromodel) performed at a constant temperature of 300 K using time step of 0.001 ps and a dielectric constant = 4.0. This procedure was followed by another sequence of CG energy minimization to a gradient threshold of < 0.1 kcal/mol/Å. Energy minimization of the complexes was performed using the AMBER all-atom force field in MacroModel. All other antagonist structures were docked inside the receptor according to the SEAL results using the CGS 15953 structure as a template.

The structures were imported in SYBYL for the superimposition procedure and for their 3D representations. The energies of the ligand–receptor complexes were 60–110 kcal/mol lower than the components. The interaction energy values were calculated as follows: ($E_{(\mathrm{ComPlex})}$) = $E_{(\mathrm{complex})} - (E_{(\mathrm{L})} + E_{(\mathrm{receptor})})$. These energies are not rigorous thermodynamic quantities but can only be used to compare the relative stabilities of the complexes. Consequently, these interaction energy values cannot be used to calculate binding affinities since changes in entropy and solvation effects are not taken into account.

2.2. Synthesis.

3,5-Dibenzyl 4-Phenylethynyl-2,6-dicy-clopropyl-1,4-dihydropyridine-3,5-dicarboxylate. Benzyl 3-oxo-3-cyclopropylpropionate (109 mg, 0.5 mmol) and ammonium acetate (77 mg, 1 mmol) in 3 mL of ethanol were heated in a sealed tube at 90 °C overnight to form benzyl 3-amino-3-cyclopropyl-2-propenoate. Phenylpropargyl aldehyde (65 mg, 0.5 mmol) and benzyl 3-oxo-3-cyclopropyl-propionate (109 mg, 0.5 mmol) were then added to this reaction system. The mixture was heated, with stirring, to 90 °C for 18 h. After cooling to room temperature, the solvent was evaporated, and the residue was purified by preparative TLC (silica 60; 1000 microns; Analtech, Newark, DE; petroleum ether-ethyl acetate 4:1) to give 54 mg of the desired product.

^{1}H NMR ($CDCl_3$, TMS): (0.053–0.72 (m, 4 H), 0.91–1.00 (m, 4 H), 2.76–2.86 (m, 2 H), 5.19 (s, 1 H), 5.27 (AB, *J* 13.8 Hz, 4 H), 5.48 (s, br, 1 H), 7.04–7.43 (m, 15 H). MS (CI–NH_3): *m/z* 547 ($M^+ + NH_4$), 530 ($M^+ + 1$), 348 ($MH^+ - 2 \times CH_2Ph$).

Anal. Calcd. for $C_{35}H_{31}NO_4$: C, 79.37; H, 5.90; N, 2.64. Found: C, 79.24; H, 5.83; N, 2.70.

Radioligand Binding Studies.—Binding of [^{3}H]/*R*-N^6-phenylisopropyladenosine ([^{3}H]*R*-PIA Amersham, Chicago, IL) to A_1 receptors from rat cerebral cortical membranes and of [^{3}H]-2-[4-[(2-carboxyethyl)phenyl]ethylamino]-5′-*N*-ethylcarbamoyladenosine ([^{3}H]CGS 21680 Dupont NEN, Boston, MA) to A_{2A} receptors from rat striatal membranes

was performed as described previously.[33,34] Adenosine deaminase (3 units/mL) was present during the preparation of the brain membranes, in a preincubation of 30 min at 30 °C, and during the incubation with the radioligands.

Binding of [^{125}I]N^6-(4-amino-3-iodobenzyl)-5′-*N*-methyl-carbamoyladenosine ([^{125}I]AB-MECA, Amersham) to membranes prepared from HEK-293 cells stably expressing the human A_3 receptor, clone HS-21a (Receptor Biology, Inc., Baltimore MD) or to membranes prepared from CHO cells stably expressing the rat A_3 receptor was performed as described.[17,35] The assay medium consisted of a buffer containing 10 mM Mg^{2+} 50 mM Tris, and 1 mM EDTA, at pH 8.0. The glass incubation tubes contained 100 μL, of the membrane suspension (0.3 mg protein/mL, stored at −80 °C in the same buffer), 50 μL of [^{125}I]AB-MECA (final concentration 0.3 nM), and 50 μL of a DMSO solution of the proposed antagonist. Nonspecific binding was determined in the presence of 100 μM N^6-phenylisopropyladenosine (*R*-PIA).

All nonradioactive compounds were initially dissolved in DMSO and diluted with buffer to the final concentration, where the amount of DMSO never exceeded *2%.*

Incubations were terminated by rapid filtration over Whatman GF/B filters, using a Brandell cell harvester (Brandell, Gaithersburg, MD). The tubes were rinsed three times with 3 mL buffer each.

At least five different concentrations of competitor, spanning 3 orders of magnitude adjusted appropriately for the IC_{50} of each compound, were used. IC_{50} values, calculated with the nonlinear regression method implemented in the InPlot program (Graph-PAD, San Diego, CA), were converted to apparent K_i values using the Cheng–Prusoff equation[36] and K_d values of 1.0 and 14 nM for [^{3}H]*R*-PIA and [^{3}H]CGS 21680, respectively, and 0.59 nM for binding of [^{125}I]AB-MECA at human A_3 receptors, respectively.

3. RESULTS

3.1. Synthesis.

As in the previous studies,[16–18] the dihydropyridine analogue was prepared through the Hantzsch condensation. This analogue was designed as the first prototypical symmetric dihydropyridine having selectivity in binding to human A_3 receptors, as predicted from recently reported structure–activity relationships (SAR). The key observations were that small cycloalkyl groups are tolerated at the 6-position, in place of a phenyl group, and benzyl esters may be present at both 3- and 5-positions.

3.2. SEAL and Electrostatic Potential Studies.

Despite the apparent structural diversity of the A_3 antagonists, certain common electronic and steric features have become apparent through the combination of computer modeling, molecular orbital calculations, potential map comparisons, and known SAR. Therefore, it was of interest to propose a hypothesis for a common mode of binding of all these different classes of A_3 antagonists. The A_3 antagonist structures analyzed in this study are shown

in Figure 1. Within each structural class, the analogue selected represents a compromise between high A_3 receptor affinity and molecular structure simplicity.

The relative comparison of the binding properties of these different A_3 antagonists requires their mutual superimposition. Previously, several molecular modeling comparisons among different agonist and/or antagonist derivatives at various subtypes of adenosine receptors have been reported.[37–43] These studies sought to maximize correlations among adenosine receptor ligands for three most important factors controlling binding to the receptor, i.e. steric, hydrophobic, and electrostatic. Different approaches to obtain structural alignments for molecular comparison have been reported.[44–46] In the present paper, we used a steric and electrostatic comparison (SEAL)[26] to align hA3ANTs structures. In this method molecules are superimposed with respect to their steric and electrostatic properties. Conformations were held rigid during the fitting procedue due to the limited degrees of freedom in these molecules. The low energy conformers of pyridine and 1,4-dihydrpyridine analogues predicted in a previous study[18] were included in the SEAL analysis. Moreover, we selected CGS 15943 as the template structure for alignment of other antagonists for the following reasons. CGS 15943, a high affinity antagonist (K_i = 14 nM) at human A_3 receptors, is conformationally restricted and nonselective. Therefore, site-directed mutagenesis results found for other adenosine receptor subtypes, in particular at the human A_1 and A_{2A} receptor, are applicable for building a hypothetical binding site also for the human A_3 receptor.

A common alignment (Figure 2) was found for all antagonist structures studied using the SEAL method with CGS 15943 as a template. This suggests that these compounds may bind at a common receptor site. The SEAL method uses the *fitting energy* to score the goodness of fit (the better the molecular fit, the lower the fitting energy). The fitting energy values are reported in Figure 2. We found a correlation between the experimentally determined K_i values at the human A_3 receptor and the corresponding fitting energies, as shown in Figure 3. This is evidence that steric and electrostatic properties of a given antagonist structure might be a useful predictor of its recognition capability in the receptor binding site environment.

As shown in Figure 2, in the first part of our analysis the properties of one of the 1,4-dihydropyridine classes of A_3 antagonists was not included. In fact, the greatest limitation in modeling structure–activity relationships in the 1,4-dihydropyridine series is that most of the derivatives reported are racemic, and there is only limited chemical and pharmacological information about the two pure enantiomers. Although analysis of nonchiral pyridine analogues can lead to a consistent model of 1,4-dihydropyridine antagonists,[18] in this study we have synthesized, a new symmetric 1,4-dihydropyridine, 3,5-dibenzyl 4-phenylethynyl-2,6-dicyclo-propyl-1,4–dihydropyridine-3,5-dicarboxylate (MRS 1496) for validation of our SEAL alignment approach. The structure and pharmacological properties of MRS 1496 are shown in Table 1. Using the SEAL/K_i correlation reported above, we have estimated a K_i value for MRS 1496 at the human A_3 receptor in the range of 100–200 nM. As reported in Table 1, the experimental K_i value is in good agreement with our prediction. These results confirm that these heterocyclic moieties can occupy the same binding site, consistent with our hypothesis for a common mode of action of the pyridine and the 1,4-dihydropyridine derivatives.

We proposed that the receptor binding properties of different A_3 antagonist derivatives are due to recognition at a common region inside the receptor binding site and, consequently, a common electrostatic potential profile. We, therefore, calculated the electrostatic contours for all A_3 antagonist derivatives, as shown in Figure 4. Though, the electrostatic potential maps present complicated topologies, it is possible to identify several regions that show a high degree of similarity among the structures. One common feature is a region of negative electrostatic potential located around the nitrogen at the 6-position of the triazoloquinazoline moiety. This region is present in all the studied antagonists and corresponds, in the xanthine series, to the 2-oxo-group of the BWA 1433 derivative and, in the pyridine series, to the carbonyl of the 5-ester group of MRS 1476 (Figure 4). These groups could hydrogen bond in the A_3 receptor–antagonist complexes. A second common feature involves the π-system of the furan and triazoloquinazoline systems. An extended aromatic system is present among all A_3 antagonist structures. A hydrophobic region corresponding to the *p*-chlorophenyl moiety of the triazoloquinazoline structure is present in the A_3 antagonists. The 6-position of the phenyl ring of the pyridine derivative, 6-position chloro of the MRS 1067 flavone structure, and the thiazolo moiety of L-268,605 show similar electrostatic potential properties in this region. Another hydrophobic region, surrounding the 1-position of the pyridine ring of MRS 1476 corresponds to the N^9-alkyl position of adenosine derivatives (agonists), which may bind to an overlapping site on the receptor. The electrostatic potential map of the 1,4-dihydropyridine derivative MRS 1496 is not represented in Figure 4, because a high degree of similarity between the corresponding electrostatic potential maps for pyridine and 1,4-dihydropyridine structures is presumed.[18]

A computer-generated model of human A_3 receptor was built and analyzed to aid in the interpretation of these SAR results.

3.3. The Antagonist Binding Site on the Human A_3 Receptor.

Fundamental understanding of the molecular details of ligand/GPCR interactions remains very rudimentary. How agonist binding transforms a resting GPCR into its active form and the microscopic basis of binding site blockade by an antagonist are generally still unclear. In the absence of high-resolution structural knowledge of GPCRs, such questions only can be addressed by building models, which are tested through pharmacological and biochemical studies. Structural models can be used to describe the interatomic interactions between a ligand and its receptor. However, even if X-ray crystal structures were available, problems would still arise in the modeling due to the dynamic nature of the ligand recognition process.[47] A bacterio-rhodopsin-based molecular model for the rat A_3 receptor was published previously.[48] We have developed an improved model of A_3 receptor interactions, using rhodopsin as a template, has been improved by adapting a facile method to simulate the reorganization of the native receptor structure induced by the ligand coordination. In fact, we have recently introduced the *cross-docking* procedure, which can be considered a further refinement in building the hypothetical binding site of A_3 receptor antagonists.[30] Details of the model building are given in the Experimental Section. Like other G protein-coupled receptor models, the length of the membrane-spanning region is about 40 Å. The interhelical distance between the pairs of adjacent helical axes is roughly 10 Å, consistent with a common interhelical contact distance.[49] The interhelical angles, measured between

the principal axes of adjacent helices, range between −150 to 170° for antiparallel and 1.0 to 25° for the parallel helices. This is typical of a 3–4 type helix–helix contact associated with optimal interactions between nearly parallel aligned helices.[49] Each helix maintained almost the same position and tilt angle after cross-docking found in the published rhodopsin 2D electron density map.[50,51] Moreover, in the cross-docked model. TM3, TM4, TM5, TM6, and TM7 were rotated clockwise 10°, 5°, 5°, 10°, and 10°, respectively, about their transmembrane axes with respect to the ligand-free receptor model. The energy of the cross-docked CGS 15943-receptor complex structure is about 80 kcal/mol lower with respect to the starting structure. Gouldson et al.[52] and More et al.[30] proposed that rotations and translations of the TM domains are crucial factors in the ligand recognition process in different GPCRs. Consequently, our approach to docking is designed to predict the natural domain reorganization within the receptors.

One of the limitations in identifying the ligand binding region of the A_3 receptor is that few site-directed mutagenesis studies have been conducted. We selected the potent but nonselective antagonist CGS 15943, as reference ligand so that site-directed mutagenesis results obtained in our laboratory for the human A_{2A} receptor could be appled to the A_3 receptor. A major structural difference between the hypothetical binding sites in these receptor subtypes is that the A_3 receptor does not contain the histidine residue in TM6 common to all A_1 (His251 in h_A_1) and A_2 (His250 in h_A_{2A}) receptors. This histidine has been shown to participate in both agonist and antagonist binding to A_{2A} receptors.[53,54] In the A_3 receptor this histidine in TM6 is replaced with a serine residue (Ser275 in h_A_3). Using the docking procedure, we identified a hypothetical binding site of CGS 15943 surrounded by TMs 3, 5, 6, and 7, with the furan ring pointing toward the extracellular environment. Figure 5A represents the minimized helical bundle following docking of CGS 15943 into the putative ligand binding cavity. In this model, the oxygen atom of Ser247 (TM7) is within hydrogen bonding distance of the N^6 atom of the triazoloquinazoline moiety at 3.8 Å. According to our site-directed mutagenesis results for the human A_{2A} receptor this serine was found to be crucial for the binding of both agonists and antagonists.[53] The NH_2 group at the 5-position of the triazoloquinazoline structure is surrounded by three polar amino acids: Ser242 (TM6), Ser271 (TM7), and Ser275 (TM7). This region seem to be very important for the recognition of antagonists. Another important interaction is predicted between the NH_2 group of Asn250 (TM6) and the oxygen of the furan ring of CGS 15943 (4.2Å). Also this asparagine residue, conserved among all adenosine receptor subtypes, was found to be important for ligand binding.[53]

A hydrophobic pocket, delimited by apolar amino acids, such as Leu90 (TM3), Phe182 (TM5), and lie 186 (TM5), is also present in the binding site model. The amino acids corresponding to Leu90 and Phe182 in the human A_{2A} receptor were found to be essential for the binding of both agonists and antagonists.[53,55] The chlorophenyl moiety of CGS 15943 is located within this region of the receptor according to our binding hypothesis. No direct interactions are predicted between the antagonist structure and the two polar amino acids Thr94 (TMS) and Ser97 (TMS). As previously reported the corresponding two amino acids in A_1 and A_{2A} receptors, respectively, are important for the coordination of agonists, but not antagonists.[53,55]

To analyze in greater detail the influence of the electrostatic potential interactions inside the trans-membrane region, we calculated electrostatic maps of three critical amino acids within the hypothetical binding site and analyzed the complementarity with the electrostatic potential of CGS 15943. As shown in Figure 6, we found a good match between the electrostatic potential generated inside the receptor and that generated by CGS 15943.

All other antagonists were docked inside the A_3 receptor model based on the SEAL results, using CGS 15943 structure as a template. Figure 5B shows the superimposition of all the docked antagonist derivatives. Strikingly, for all the antagonist structures included in the present study, complementary interactions with the receptor are evident, such as hydrogen bonding with Ser247 (TM7), interaction with Asn250 (TM6), and the hydrophobic region around Leu90 (TM3), Phe182 (TMS), and Ile186 (TM5), as shown in Figure 7.

4. CONCLUSION

In conclusion, this theoretical study supports the hypothesis of a common mode of action for hA3ANTs and emphasizes the importance of the electrostatic potential interactions in the receptor–ligand recognition process. This is consistent with the competitive behavior of these different classes of antagonists at the human A_3 receptor. Understanding the pharmacophore requirements of the A_3 receptor may lead to the rational design of new active compounds, as we have recently demonstrated with the discovery of the class of pyridine derivative A_3 antagonists.

ACKNOWLEDGMENT

The authors are grateful for helpful comments and encouragement provided by Dr. Robert Pearlstein of the Center for Molecular Modeling (CIT), NIH. We thank Dr. Neli Melman of Molecular Recognition Section (NIDDK/LBC), NIH for determination of K_i values for MRS 1496.

REFERENCES AND NOTES

(1). Jacobson KA; van Rhee AM Development of selective purinoceptor agonists and antagonists. In purinergic Approaches in Experimental Therapeutics; Jacobson KA, Jarvis MF, Eds.; Wiley: New York, 1997; Chapter 6, pp 101–128.

(2). Ramkumar V; Stiles GL; Beaven MA; Ali H The A_3 adenosine receptor is the unique adenosine receptor which facilitates release of allergic mediators in mast cells. J. Biol. Chem. 1993, 268, 16887–16890. [PubMed: 8349579]

(3). Ali H; Choi OH; Fraundorfer PF; Yamada K; Gonzaga HMS; Beaven MA Sustained activation of phospholipase-D via adenosine A_3 receptors is associated with enhancement of antigenionophore-induced and Ca^{2+}-ionophore-induced secretion in a rat mastcell line. J. Pharmacol. Exp. Therap. 1996, 276, 837–845. [PubMed: 8632357]

(4). Jacobson KA; Kim HO; Siddiqi SM; Olah ME; Stiles G von Lubitz DKJE A_3 adenosine receptors: design of selective ligands and therapeutic prospects. Drags of the Future 1995, 20, 689–699.

(5). von Lubitz DKJE; Lin RCS; Popik P; Carter MF; Jacobson KA Adenosine A_3 receptor stimulation and cerebral ischemia. Eur. J. Pharmacol. 1994, 263, 59–67. [PubMed: 7821362]

(6). von Lubitz DKJE; Lin RC-S; Jacobson KA Adenosine A_3 receptor antagonists and protection against cerebral ischemic damage in gerbils. Soc. Neurosci. Abstract 1997, 23, 1924.

(7). Beaven MA; Ramkumar V; Ali H Adenosine-A_3 receptors in mast-cells. Trends Pharmacol. Sci. 1994, 15, 13–14.

(8). Knight D; Zheng X; Rocchini C; Jacobson MA; Bai T; Walker B Adenosine A_3 receptor stimulation inhibits migration of human eosinophils. J. Leukoc. Biol. 1997, 62, 465–468. [PubMed: 9335316]

(9). Ali H; Muller CE; Daly JW; Beaven MA Methylxanthines block antigen-induced responces in RBL-2H3 cells independently of adenosine receptors or cyclic AMP: evidence for inhibition of antigen binding to IgE. J. Pharmacol. Exp. Ther. 1991, 258, 954–962. [PubMed: 1716313]

(10). Zhou QY; Li CY; Olah MF; Johnson RA; Stiles GL; Civelli O Molecular cloning and characterization of an adenosine receptor – The A_3 adenosine receptor. Proc. Natl. Acad. Sci. U.S.A. 1992, 89, 7432–7436. [PubMed: 1323836]

(11). Salvatore CA; Jacobson MA; Taylor HE; Linden J; Johnson RG Molecular cloning and characterization of the human A_3 adenosine receptor. Proc. Natl. Acad. Sci. U.S.A. 1993, 90, 10365–10369. [PubMed: 8234299]

(12). Camaioni E; Costanzi S,; Viitori S; Volpini R; Klotz K-N; Cristalli G Adenosine receptor antagonists: new purine derivatives. Bioorg. Med. Chem. 1998, 6, 523–533. [PubMed: 9629466]

(13). Karton Y; Jiang JI,,; Ji XD; Melman N; Olah ME; Stiles GL; Jacobson KA Synthesis and biological-activities of flavonoid derivatives as as adenosine receptor antagonists. J. Med. Chem. 1996, 39, 2293–2301. [PubMed: 8691424]

(14). Francis JE; Cash WD; Psychoyos S; Ghai G; Wenlc P; Friedmann RC; Atkins C; Warren V; Furness P; Hyun JL Structure - activity profile of a series of novel triazoloquinazoline adenosine antagonists. J. Med. Chem. 1988, 31, 1014–1020. [PubMed: 3361572]

(15). Kim Y-C; Ji X.d.; Jacobson KA Derivatives of the triazoloquinazoline adenosine antagonist (CGS15943) are selective for the human A_3 receptor subtype.,J. Med. Chem. 1996, 39, 4142–4148. [PubMed: 8863790]

(16). van Rhee AM; Jiang J Melman N; Olah ME; Stiles GL; Jacobson KA Interaction of 1,4-dihydropyridine and pyridine-derivatives with adenosine, receptors-selectivity for At receptors. J. Med. Chem. 1996, 39, 2980–2989, [PubMed: 8709132]

(17). Jiang J.-l.; van Rhee AM; Melman N; Ji X.d.; Jacobson K A. 6-Phenyl-1,4-dihydropyridine derivatives as potent and selective A_3 adenosine receptor antagonists. J. Med. Chem. 1996, 39, 4667–4675. [PubMed: 8917655]

(18). Li A-H; Moro S; Melman N; Ji X.-d.; Jacobson KA Structure activity relationships and molecular modeling of 3,5-diacyl-2,4-dialkylpyridinederivatives as selective A_3 adenosine receptor antagonists J. Med. Chem. 1998, 41, 3186–3201. [PubMed: 9703464]

(19). Jacobson MA; Chakravarty PK.; Johnson, R. G.; Norton, R. Novel selective nonxanthine selective A_3 adenosine receptor antagonists. Drug Devel. Res. 1996, 37, 131.

(20). Tile program SYBYL 6.3 is available from TRIPOS Associates, St. Louis, MO, 1993.

(21). Dewar MJSE; Zoebisch G; Healy EF AMI: A New General Purpose Quantum Mechanical Molecular Model. J. Am. Chem. Soc. 1985, 107, 3902–3909.

(22). MOPAC 6.0 is available from Quantum Chemistry Program Exchange.

(23). Gaussian 94, Revision C.2; Frisch MJ; Trucks GW; Schlegel HB; Gill PMW; Johnson BG; Robh MA; Cheeseman JR; Keith T; Petersson GA; Montgomery JA; Raghavachari K; Al-Laham MA; Zakrzewski VG; Ortiz JV; Foresman JB; Cioslowski J; Stefanov BB: Nanayakkara A; Challacombe M; Peng CY; Ayala PY; Chen W; Wong MW; Andres IL; Replogle ES; Gomperts R; Martin RL; Fox DJ; Binkley JS; Defrees D; Baker JJ; Stewart JP; Head-Gordon M; Gonzalez C; Pople JA Gaussian, Inc., Pittsburgh, 1995.Dobbs KD; Hehre WJ Molecular orbital theory of the properties of inorganic and organometallic compounds 5. Extended basis sets for first-row transition metals. J. Comput. Chem. 1987, 8, 861–879.

(24). Dobbs KD; Hehre WJ Molecular orbital theory of the properties of inorganic and organometallic compounds 5. Extended basis sets for first-row transition metals. J. Comput. Chem. 1987, 8, 861–879.

(25). Chirlian LE; Francl MM Atomic charges derived from electrostatic potentials: a detailed study. J. Comput. Chem. 1987, 8, 894–905.

(26). Kearsley SK; Smith GM An Alternative Method for the Alignment of Molecular Structures: Maximizing Electrostatic and Steric Overlap. Tetrahedron Comput. Methodol. 1990, 3, 615–633.

(27). The program PowerFit v.1.0 is available from MicroSimulations, 478 Green Mountain Road, Mahwah, NJ 07430, 1996.

(28). Mohamadi F; Richards NGJ; Guida WC; Liskamp R; Lipton M; Caufield C; Chang G; Hendrickson T; Still WC Macro-Model-An Integrated Software System for Modeling Organic and Bioorganic Molecules using Molecular Mechanics. J. Comput. Chem. 1990, 11, 440–450.

(29). van Rhee AM; Fischer B; van Galen PJM; Jacobson KA Modelling the P2Y purinoceptor using rhodopsin as template. Drug Design Discovery 1995, 13, 133–154. [PubMed: 8872457]

(30). Moro S; Guo D; Camaioni E,; Boyer JL; Harden KT: Jacobson KA Human P2Y1 receptor: molecular modeling and site-directed mutagenesis as tools to identify agonist and antagonist recognition sites. J. Med. Chem. 1998, 41, 1456–1466. [PubMed: 9554879]

(31). Kyte J; Doolittle RF A simple method for displaying the hydrophobic character of a protein. J. Mol. Biol. 1982, 157, 105–132. [PubMed: 7108955]

(32). Weiner SJ; Kollman PA; Nguyen DT; Case DA An all-atom force field for simulation of protein and nucleic acids. J. Comput, Chem. 1986, 7, 230–252. [PubMed: 29160584]

(33). Schwabe U; Trost T Characterization of adenosine receptors in rat brain by (–) [^{3}H]N^{6}-phenylisopropyladenosine. Naunyn-Schmiede-berg's Arch. Pharmacol. 1980, 313, 179–187.

(34). Jarvis MF; Schütz R; Hutchison AJ; Do E; Sills MA; Williams M [^{3}H]CGS 21680, an Ao selective adenosine receptor agonist directly labels A2 receptors in rat brain tissue. J. Pharmacol. Exp. Therap. 1989, 251, 888–893. [PubMed: 2600819]

(35). Olah ME; Gallo-Rodriguez C; Jacobson KA; Stiles GL [^{125}I]-AB-MECA, a high affinity radioligand for the rat A_3 adenosine receptor. Mol. Pharmacol. 1994, 45, 978–982. [PubMed: 8190112]

(36). Cheng YC; Prusoff WH Relationship between the inhibition constant (Ki)) and the concentration of inhibitor which causes 50% inhibition (IC_{50}) of an enzyme reaction. Biochem. Pharmacol. 1973, 22, 3099–3108. [PubMed: 4202581]

(37). Galen P. J. M. v.; Vlijmen H. W. T. v.; IJzerman AP; Soudijn W A model for the antagonist binding site on the adenosine A_1 receptor, based on steric, electrostatic, and hydrophobic properties. J. Med. Chem. 1990, 33, 1708–13. [PubMed: 2342066]

(38). Peet NP; Lentz NL; Meng EC; Dudley MW; Ogden AM; Demeter DA; Weintraub HJ; Bey P A novel synthesis of xanthines: support for a new binding mode for xanthines with respect to adenosine at adenosine receptors. J. Med. Chem. 1990, 33, 3127–3130. [PubMed: 2258897]

(39). Dooley MJ; Quinn RJ The Three Binding Domain Model of Adenosine Receptors Molecular Modeling Aspects. J. Med. Chem. 1992, 35, 211–216. [PubMed: 1732538]

(40). Quinn RJ; Dooley MJ; Escher A; Harden FA; Jayasuriya H A Computer Generated Model of Adenosine Receptors Rationalising Binding and Selectivity of Receptor Ligands. Núcleos. Nucleot. 1991, 10, 1121–1124.

(41). van Rhee AM; Siddiqi SM; Melman N; Shi D; Padgett WL; Daly JW; Jacobson KA Tetrahydrobenzothiophenone derivatives as a novel class of adenosine receptor antagonists. J. Med. Chem. 1996, 39, 398–406. [PubMed: 8558508]

(42). Dooley MJ; Kono M; Suzuki F Conformational search for the N^{6}-substituted adenosine analogues and related adenosine A_1 receptor antagonists. Bioorg. Med. Chem. 1996, 4, 917–921. [PubMed: 8818242]

(43). Dooley MJ; Kono M; Suzuki F Theoretical structure–activity studies of adenosine A_1 ligands: requirements for receptor affinity. Bioorg. Med. Chem. 1996, 4, 923–934. [PubMed: 8818243]

(44). Humblet C; Marshall GR Pharmacophore identification and receptor mapping. Ann. Rep. Med. Chem. 1980, 15, 267–276.

(45). Hopfinger AJ Computer-assisted drug design. J. Med. Chem. 1985, 28, 1133–1139. [PubMed: 2993608]

(46). Gund Andese, Rhodes JD, J. B.; Smith GM Three-dimensional molecular modeling and drug design. Science 1980, 208, 1425–1431. [PubMed: 6104357]

(47). Herzyk P; Hubbard RE Automated method for modeling seven-helix transmembrane receptors from experimental data. Biophys. J. 1995, 69, 2419–2442. [PubMed: 8599649]

(48). van Galen PJM; van Bergen AH; Gallo-Rodriguez C; Melman N; Olah ME: IJzerman AP; Stiles GL; Jacobson KA A binding site model and structure–activity relationships for the rat A_3 adenosine receptor. Mol, Pharmacol. 1994, 45, 1101–1111. [PubMed: 8022403]

(49). Chiota C; Icvitt M; Richardson D Helix to helix packing in proteins. J. Mol. Biol. 1981, 145, 215–250. [PubMed: 7265198]

(50). Schertler GF; Villa C; Henderson R Projection structure of rhodopsin. Nature 1993, 362, 770–772. [PubMed: 8469290]

(51). Urger VM; Hargrave PA; Baldwin JM; Schertler GFX Arrangement of rhodopsin transmenbrane α-helices. Nature 1997,389, 203–206. [PubMed: 9296501]

(52). Gouldson PR; Snell CR; Reynolds CA A new approach to docking in the b2-adrenergic receptor that exploits the domain structure of G protein-coupled receptors. J. Med. Chem. 1997,40, 3871–3886. [PubMed: 9397168]

(53). Kim J; Wess J; van Rhee AM; Shoneberg T; Jacobson KA Site-directed mutagenesis identifies residues involved in ligand recognition in the human A_{2a} adenosine receptor. J. Biol. Chem. 1995, 270, 13987–13997. [PubMed: 7775460]

(54). Jiang Q, Lee BX, Glashofer M, van Rhee AM, and Jacobson KA Mutagenesis reveals structure–function parallels between human A_{2A}-adenosine receptors and the biogenic amine family. J. Med. Chem. 1997, 40, 2588–2595. [PubMed: 9258366]

(55). Jiang Q; van Rhee AM; Kim J; Yehle S; Wess J; Jacobson KA Hydrophilic side chains in the third and seventh transmembrane helical domains of human A_{2a} adenosine receptors are required for ligand recognition. Mol. Pharmacol. 1996, 50, 512–521. [PubMed: 8794889]

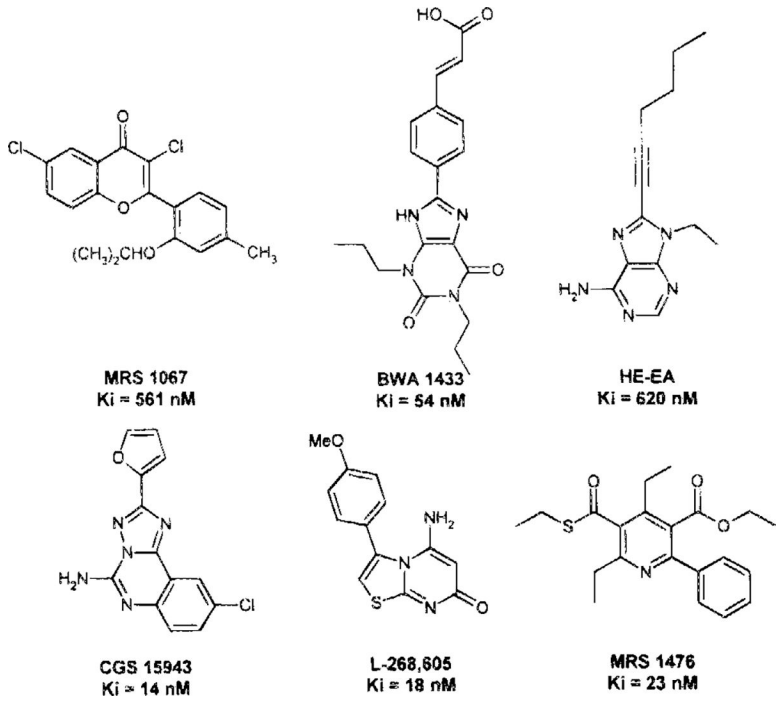

Figure 1.

Structures of A_3 receptor selective antagonist of diverse chemical structures. K_i values (nM) for the binding of human A_3 receptor are shown.

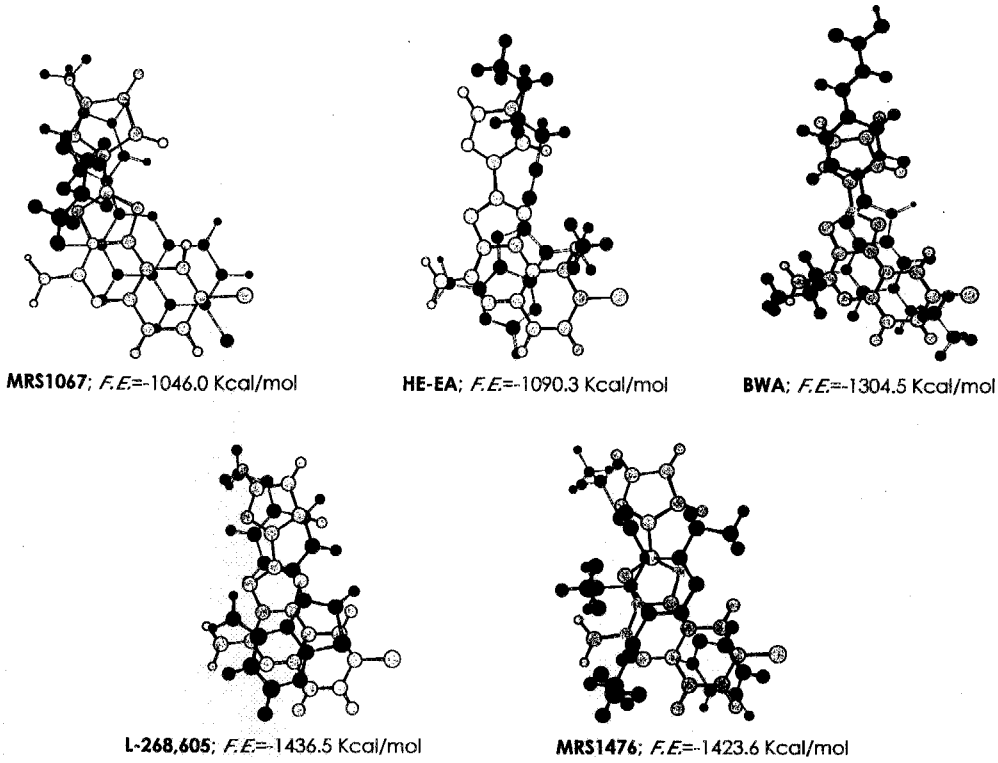

Figure 2.

Alignments generated by SEAL using CGS 15943 as reference structure (colored in gray). The fitting energy values (*F.E.*, kcal/mol) are given alongside each superimposed pair.

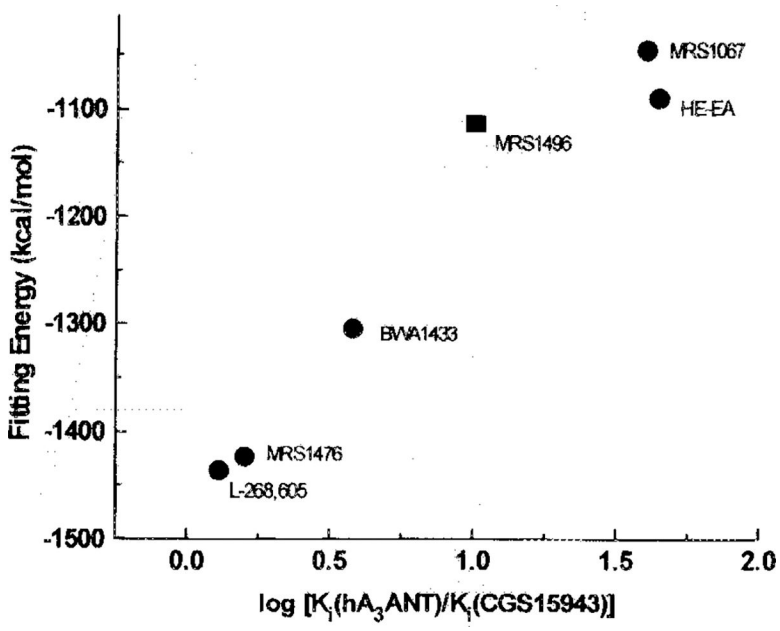

Figure 3.

Correlation between the fitting energy values (*F.E.*, kcal/mol) obtained using the SEAL algorithm and the log[K_i(hA3ANT)/K_i(CGS 15943)] values. The MRS 1496 *F.E.* (square marker) was used to predict its K_i value.

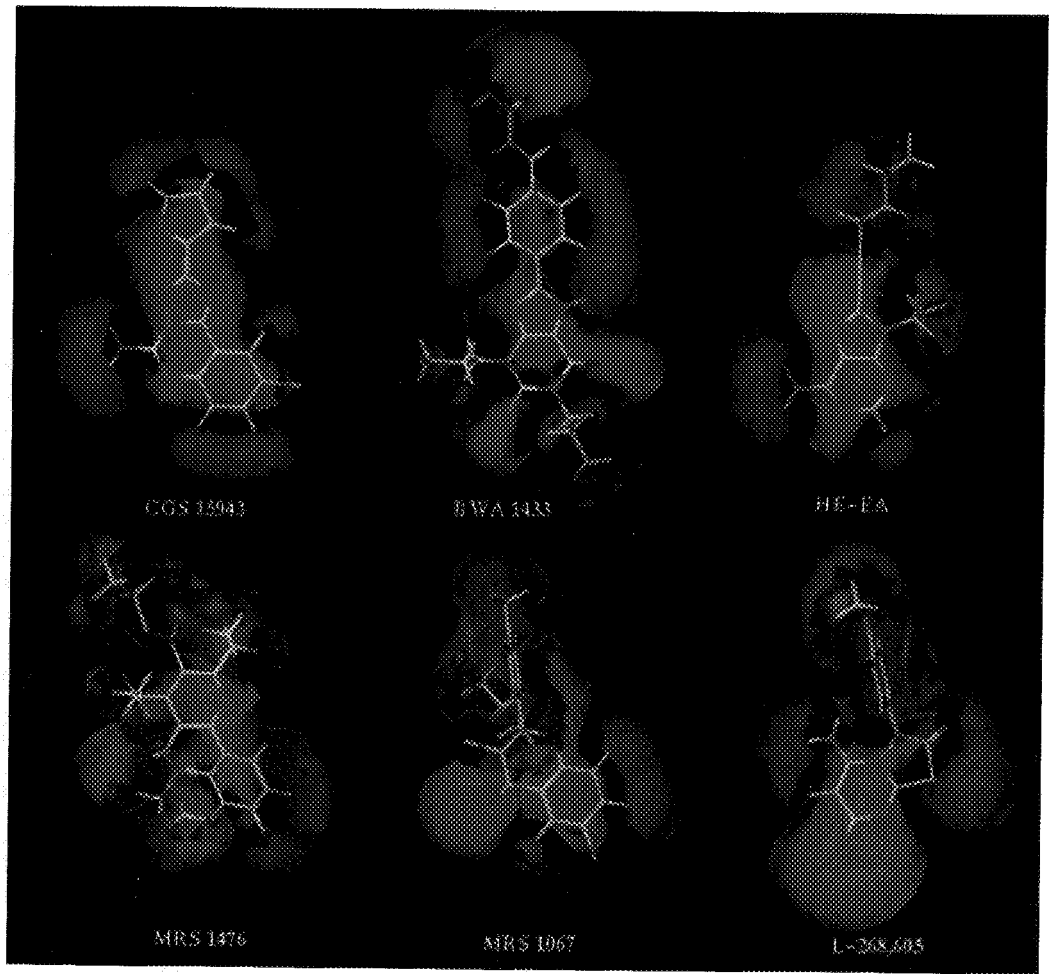

Figure 4.
Comparison between the isopotential surface of different A_3 receptor antagonist structures, (red = 5.0 kcal/mol, and blue = −5.0 kcal/mol).

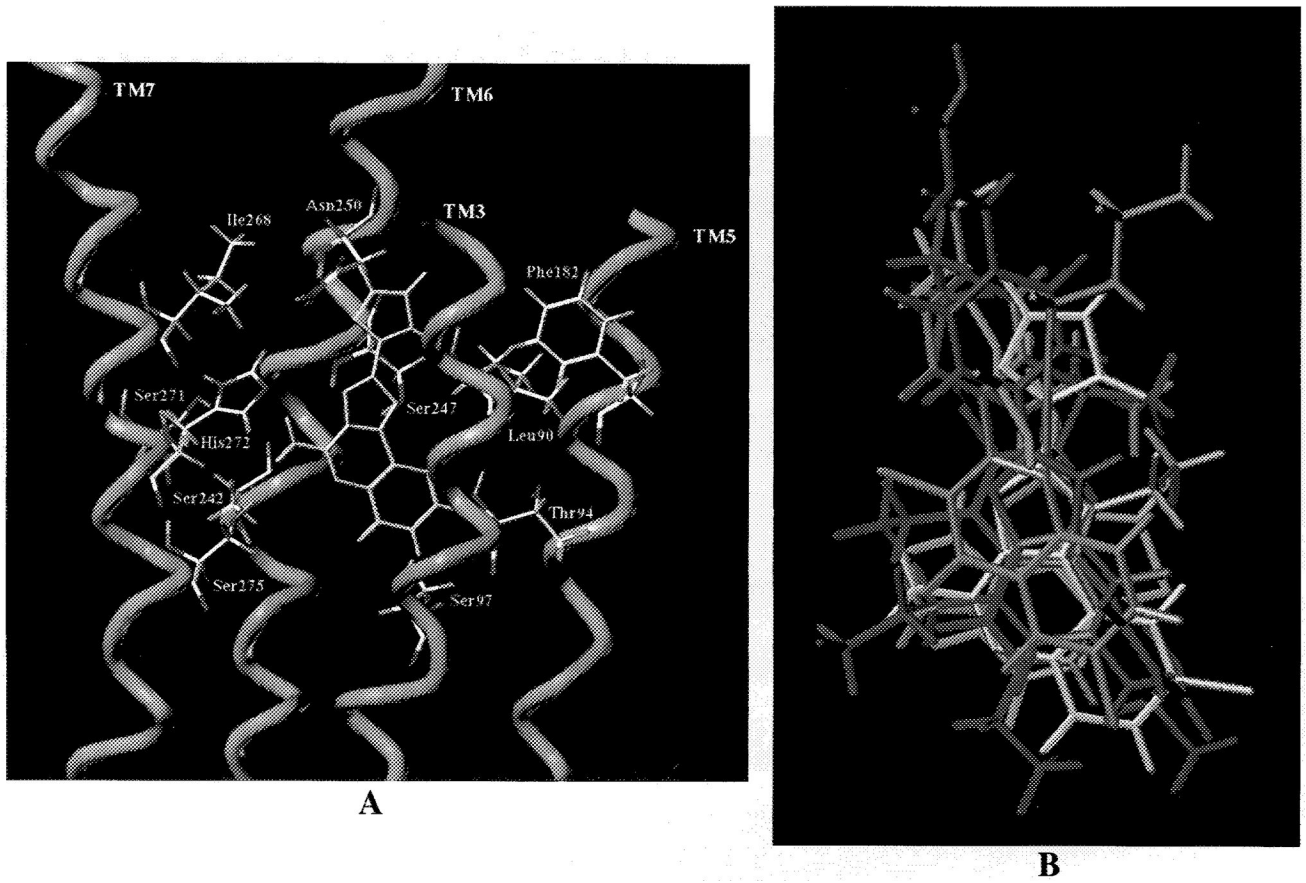

Figure 5.

(A, left) Side view of the A_3–CGS 15943 complex model. The side chains of the important residues in proximity to the docked CGS 15943 molecule are highlighted and labeled. Residues in proximity (≤5 Å) to the docked CGS15943 molecule: Leu90 (TM3), Phe182 (TM5), Ser242 (TM6), Ser247 (TM6), Asn250 (TM6), Ser271 (TM7), His272 (TM7), Ser275 (TM7). (B, right) Superposition of all docked A_3 antagonist structures. The transmembrane helical bundle is not highlighted, but it conserves the same arrangement shown in Figure 5A. Blue = MRS 1476; green = L-268,605; yellow = CGS 15943; magenta = MRS 1067; orange = HE-EA.

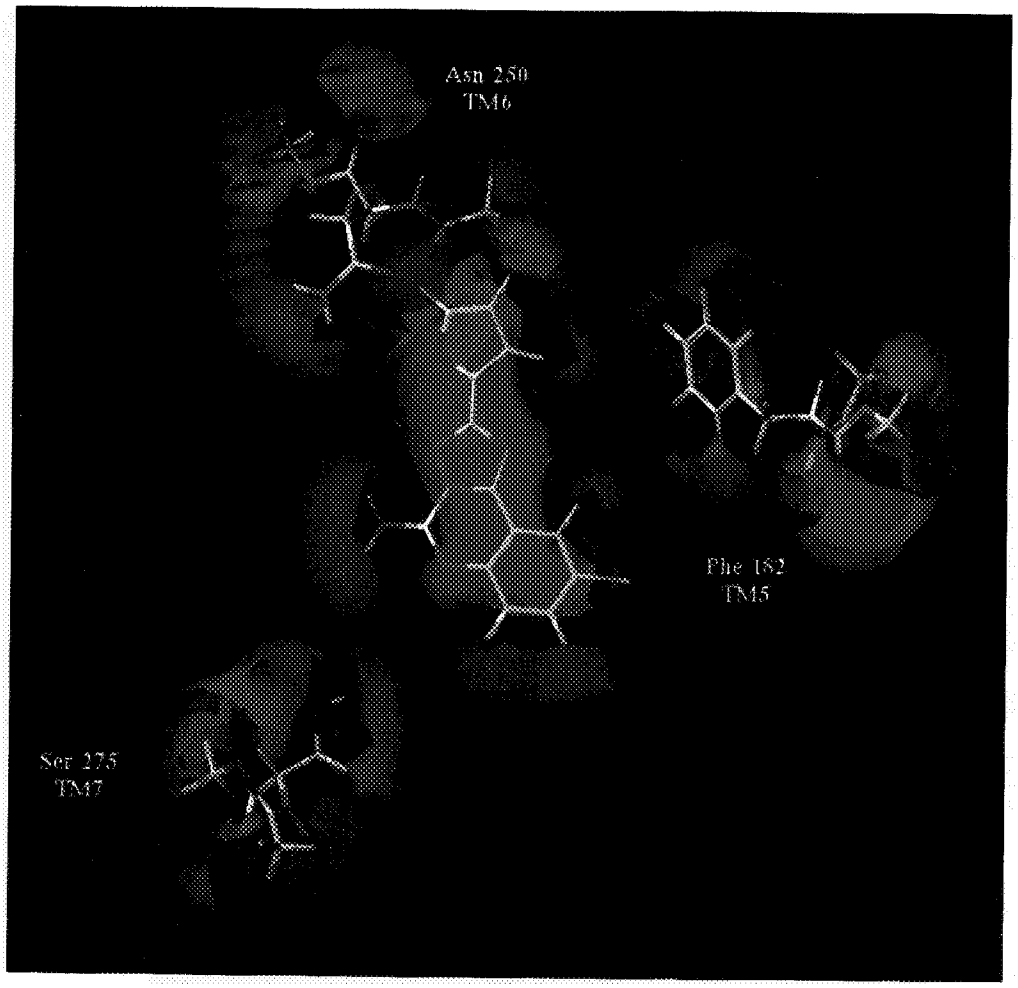

Figure 6.

Isopotential surface of docked CGS 15943 structure and of three important amino acids located in proximity of the antagonist structure: Phe182 (TM5), Asn250 (TM6). and Ser275 (TM7) (red = 5.0 keal/mol, and blue = −5.0 kcal/mol).

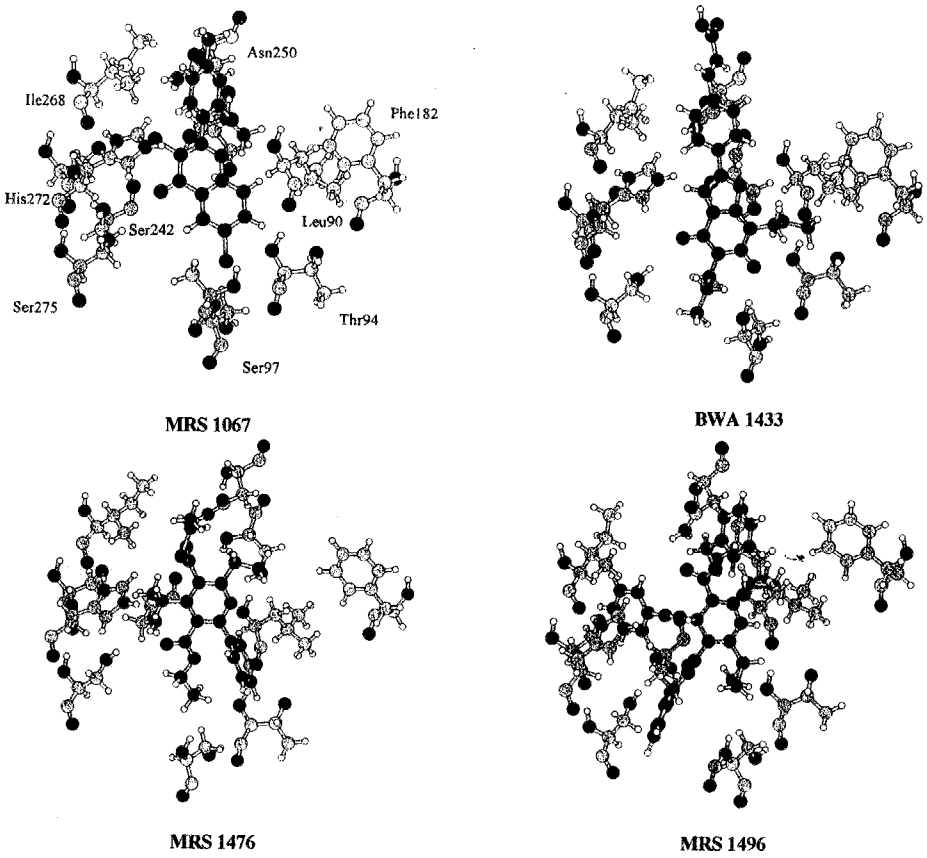

Figure 7.

Table 1.

Affinity of MRS 1496 in Radioligand Binding Assay at A_1, A_{2A}, and A_3 Receptors

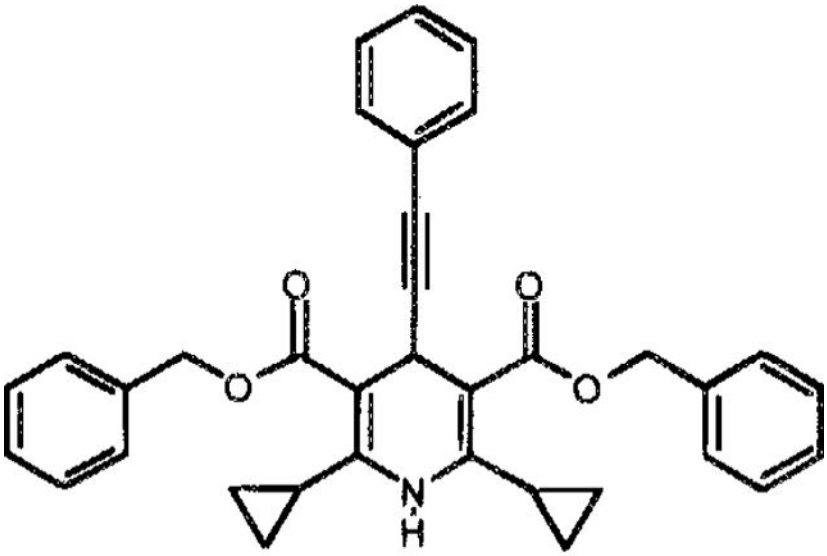

MRS 1496

ligand	(*r*)A_1 receptor[a] binding affinity K_i (*μ*M)	(*r*)A_{2A} receptor[b] binding affinity % displacement (10^{-4} M)	(*h*)A_3 receptor[c] binding affinity K_i (μM)
MRS 1496	15.8 ± 1.9	23 ± 10%	0.251 ± 0.028

[a]Displacement of specific [^{3}H]*R* – PIA binding in rat brain membranes, expressed as K_i ± SEM (*n* = 4).

[b]Percentage of specific binding of [^{3}H]CGS 21680 in rat striatal membranes displaced at the indicated concentration (*n* = 2).

[c]Displacement of specific [^{125}I]AB-MECA binding in membranes of HEK293 cells expressing the human A3 receptor, expressed as K_i ± SEM (*n* = 4).